Geothermics 90 (2021) 101999

Contents lists available at ScienceDirect

Geothermics

journal homepage: www.elsevier.com/locate/geothermics

Regional-scale assessment of the thermal potential in a shallow alluvial aquifer system in the Po plain (northern Italy)

Alberto Previati *, Giovanni B. Crosta

DISAT – Department of Earth and Environmental Sciences, University of Milano Bicocca, Piazza della Scienza, 4, Milan, 20126, Italy

ARTICLE INFO

Keywords:
Regional-scale thermal potential
Shallow geothermal energy
Ground-coupled heat pumps
Groundwater heat pumps
Milan metropolitan area

ABSTRACT

The Milan Metropolitan Area is one of the most densely populated regions in Italy and Europe and, consequently, has an extremely high thermal power demand. In this study a regional scale assessment of the potential of a shallow alluvial aquifer to host low enthalpy geothermal systems is presented. The study area lies on a layered phreatic aquifer complex and presents advantageous hydrogeological characteristics that make low enthalpy geothermal supply an attractive heating/cooling solution from a carbon footprint and an economical point of view. In this context, different analytical solutions were used to estimate the thermal potential of closed- and open-loop systems based on the distribution of hydraulic and thermal parameters of the shallow aquifers. The thermal potential of closed-loop systems (ground-coupled heat pumps - GCHP) was estimated through the ASHRAE analytical equation considering the hydraulic and thermal parameters of the ground, the groundwater temperature, and the characteristics of the system. The thermal potential of open-loop systems (groundwater heat pumps - GWHP) was estimated by considering the local regulation on the abstraction and the conservation of the quantity and the quality of the groundwater as well as preventing excessive groundwater table drawdown or rising and thermal short-circuit. The results were compared with heat demand rates of the buildings in the municipalities of the study area and, finally, the most profitable shallow geothermal system configuration is discussed.

1. Introduction

The European commitment on climate change mitigation and decarbonization focuses on ambitious and promising goals such as [1] reaching a share of at least 32 % of renewable energy by 2030 (European Commission, 2018) and [2] reducing greenhouse gas emissions to 80–95 % below 1990 levels by 2050 (European Climate Foundation, 2010). Low enthalpy shallow geothermal energy is considered a valid alternative to common carbon-based heating/cooling techniques (e.g. fossil fuel burners, air-coupled heat pumps) (Lund and Boyd, 2016). Even though shallow geothermal systems require electricity to extract heat from the ground, a significantly lower amount of electrical power is required and lower volumes of greenhouse gases (GHGs) are emitted if compared to conventional heating/cooling systems (Blum et al., 2010). It has been demonstrated that the use of geothermal energy in common residential and commercial buildings in Europe can reduce the emission of GHGs, such as CO_2, between 31 % and 88 % (depending on the source of the supplied electricity and the efficiency of the installation) compared to conventional heating systems such as oil and gas fired boilers and air-coupled heat pumps (Saner et al., 2010). Moreover, low enthalpy geothermal systems have proved to be the best cost-effective conditioning solution for a wide range of buildings, notwithstanding the high initial investment costs (Self et al., 2013).

Low enthalpy shallow geothermal systems can be subdivided into two main categories:

- **Ground-coupled heat pumps (GCHP–Closed-Loop):** the heat transfer fluid circulates in a loop placed in the ground with which it has no direct contact. The heat transfer with the ground occurs through the piping material.
- **Groundwater heat pumps (GWHP–Open-Loop):** the heat is carried directly with the groundwater by passing directly through the heat exchanger. After the heat exchange the water is given back to the aquifer or to surface water bodies.

In Italy, the low-enthalpy geothermal energy annual production (2756 GW h in 2017 (GSE, 2018)) still accounts for only 0.4 % of the total thermal energy production and represents about 2% of the

* Corresponding author.
E-mail address: a.previati1@campus.unimib.it (A. Previati).

https://doi.org/10.1016/j.geothermics.2020.101999
Received 5 June 2020; Received in revised form 22 October 2020; Accepted 9 November 2020
Available online 26 November 2020
0375-6505/© 2020 The Authors. Published by Elsevier Ltd. This is an open access article under the CC BY-NC-ND license

renewable thermal energy production (GSE, 2018). However, a continuously increasing trend has been observed since 2012 (+8 % in 5 years) (GSE, 2018), and a strong rise of about 300 % is expected within 2030 (Unione Geotermica Italiana, 2017).

The most severe obstacles to the use of geothermal heat pumps are the high initial investment cost due to the drilling and installation procedures, and the high cost of domestic electricity (0.21 €/kWh) compared to methane (0.08 €/kWh) (EUROSTAT, 2019). To account for these economic limitations the Italian public authorities introduced a tax relief up to 65 % of the investment amount for energy-renovation of existing buildings (ENEA, 2018). Moreover, the Italian energy regulation on new buildings *(D.Lgs. 28/2011)* states that at least 50 % of the thermal energy used for space heating and cooling (and for hot water supply) must come from renewable sources.

Another common obstacle is the lack of knowledge of the potential of this heating/cooling technique and about the sites where they can be more efficiently and easily installed. One of the best indicators of geothermal efficiency and suitability is the geothermal potential. Even though it is not uniquely defined (Bayer et al., 2019), the geothermal potential depicts the capability to exchange heat with the ground or the groundwater.

Bayer et al. (2019) reviewed the most relevant works on the geothermal potential assessment introducing the distinction between the theoretical potential (i.e. the total energy stored in a reservoir or the amount of exchangeable heat based only on the hydrogeological and thermal properties of the exploitable aquifers) and the technical potential (i.e. the fraction of the theoretical potential that can be used by a certain technology). In practice only a fraction of the theoretical potential can be exploited depending on technical restrictions and on the existing regulations about the conservation of the groundwater resources, and the protection of the thermal status of the aquifers. In this context, a comprehensive assessment of the thermal potential taking into account the hydrogeological and thermal settings (i.e. the hydraulic and thermal properties of each unit and the present thermal regime), and the restrictions imposed by local regulations, is needed to define the effective technical potential.

Many authors mapped the technical geothermal potential of GCHPs and GWHPs by combining climatic and thermo-geological information through theoretical physical equations (García-Gil et al., 2015; Zhu et al., 2011) or empirical equations (Böttcher et al., 2019; Casasso and Sethi, 2016; Galgaro et al., 2015; Viesi et al., 2018) and derived techno-economic indicators such as the investment cost and payback times (Perego et al., 2019). At the city scale Epting et al. (2018) and Mueller et al. (2018) evaluated the amount of extractable heat through numerical modeling techniques. These methods are very precise tools for city-scale geothermal potential assessment and thermal management of local aquifers but are computationally expensive for regional-scale geothermal mapping.

The objective of this study is to characterize the low enthalpy geothermal potential for closed- and open-loop systems for an intensively urbanized and industrialized portion of the Po plain (northern Italy) by linking geological and hydrogeological information to climatic data, and to discuss the potential of this fast-growing area to fulfill the extensive heating/cooling demand as well as to define which is the best technology according to the hydrogeological framework and heat demand scenarios.

In this context, a GIS-based procedure was applied according to the following steps: (i) collection and homogenization of stratigraphic information as from borehole logs, (ii) assignment of hydraulic and thermal properties to the lithological units, (iii) estimate of the equivalent properties for different depth intervals, (iv) mapping of hydrogeological parameters and aquifer temperature, (v) application of analytical equations to derive the technical thermal potential, and (vi) discussion of the results by comparing the actual thermal energy demand of the municipalities in the study area.

2. Study area

The study area is located in the northern portion of the Po plain (northern Italy) and is bounded by the Adda, Ticino and Po rivers eastward, southward and westward, respectively, and by the alpine foothills to the north (Fig. 1). The area covers 3,827 km^2 and is one of the most densely populated (5,351,148 inhabitants) and industrialized regions in Italy (mean population density: 1398 inhabitants/km^2, max: 6,836 inhabitants/km^2 in the city of Milan) (ISTAT, 2019). This area has a great potential for shallow geothermal exploitation due to its advantageous hydrogeological settings (e.g. the equivalent horizontal hydraulic conductivity of the phreatic aquifer ranges between $5*10^{-5}$ and $1*10^{-2}$ m/s and the average saturated thickness is about 40 m) and due to the high heating/cooling demand.

2.1. Climate

The climate of the study area is overall homogeneous since the elevation ranges between 40 and 400 m a.s.l. According to the Köppen-Geiger classification (Rubel et al., 2017) the climate regime falls between the Cfa (i.e. warm-temperate, humid with hot summers) and Csb classes (i.e. warm-temperate with warm and dry summers), and it is typically continental with moderately cold winters and hot muggy summers. The mean annual precipitation varies between 800 and 1000 mm/yr (ARPA Lombardia, 2019).

According to the meteorological records of the last 20 years, the mean annual air temperature is about 14.2 °C with a minimum mean daily temperature of -5.4 °C and a maximum mean daily temperature of +31 °C (ARPA Lombardia, 2019). These values are approximately constant in the whole study area, even if warmer conditions can be found in the Milan urban area due to the heat island effect (Pichierri et al., 2012). This phenomenon is reflected by a mean annual air temperature of about 15.7 °C recorded by the meteorological monitoring station located in the center of Milan (ARPA Lombardia, 2019) that is 2 °C higher than the nearest available air temperature measurement outside the city (see also Fig. 6).

Due to the mild continental climate, the buildings in the study area need both heating and cooling. The amount of thermal energy required for heating or cooling depends on the degree days. Degree days were estimated as the difference between the air temperature and the reference indoor temperature below (or above) which a building will require active heating (or cooling). Annual heating degree days range between 1800 and 2300, whereas cooling degree days range from 400 to 800 (see also Section 3.1.3).

2.2. Geology and hydrogeology

The northern portion of the Po plain forms the foreland basin of the Alpine collisional belt hosting a sequence of deposits up to 800 m thick characterized by deep marine sediments, covered by fluvioglacial sequences relative to the onset of major glaciations and by the progradation of laterally extensive alluvial sediments coming from the Alps (Garzanti et al., 2011; ISPRA and Regione Lombardia, 2016; Regione Lombardia and ENI Division Agip, 2002).

The various depositional events from early Pleistocene account for the creation of three main depositional sequences (Fig. 2) which correspond to as many aquifer complexes (from top to bottom):

(I) Unconfined aquifer (Aquifer Group A, Regione Lombardia and ENI Division Agip, 2002): mainly consists of gravel with a sandy matrix. The aquifer, 20–50 m thick, overlays a clayey silty regional aquitard (0.45 Ma) which shows a good continuity south of Milan, and disappears moving northward. (II) Semi-confined aquifer (Aquifer Group B, Regione Lombardia and ENI Division Agip, 2002): consists of sands and sandy gravels with a thickness in the range between 50 m and 100 m. The lower portion of the aquifer consists of clay and silt layers, and locally of conglomeratic units (i.e. Ceppo formation). The major

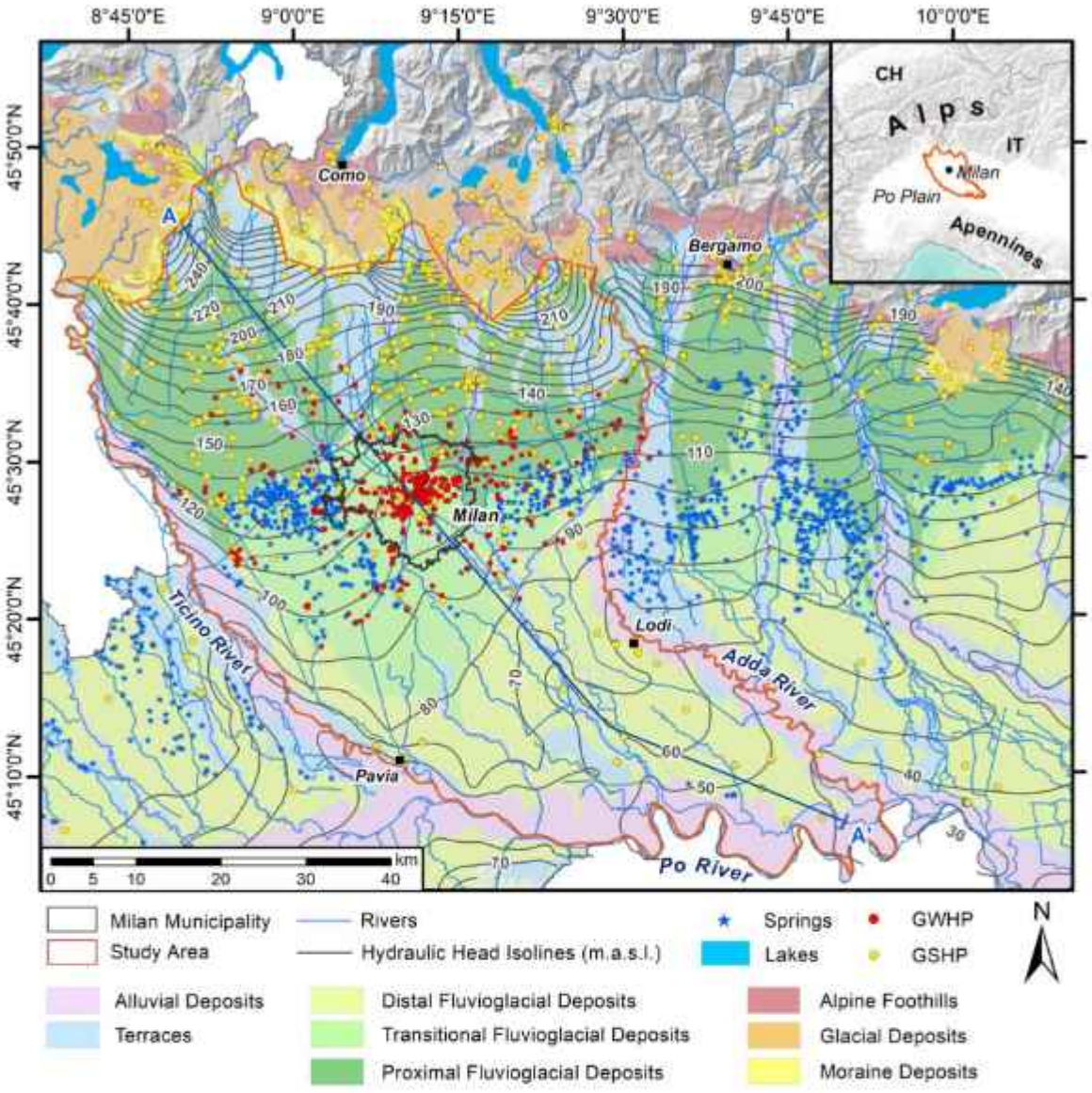

Fig. 1. Map of the study area showing the distribution of the shallow deposits and the hydrological network. (For interpretation of the references to colour in the figures, the reader is referred to the web version of this article).

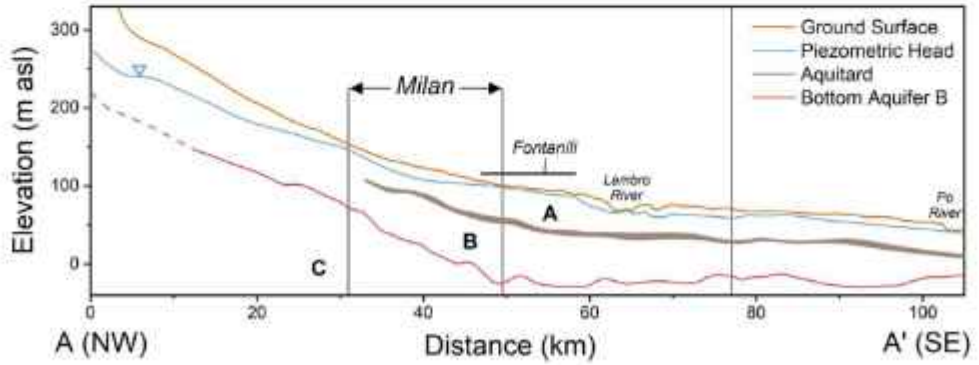

Fig. 2. Simplified cross-section profile showing the boundary surfaces between the three main regional aquifers in the study area, from top to bottom: phreatic (A), semi-confined (B) and confined (C).

Pleistocene glaciations in the Alps produced a widespread sequence boundary in the basin at 0.87 Ma. (III) Deep confined aquifer (Aquifer Group C, Regione Lombardia and ENI Division Agip, 2002): consists of clay and silt units with sandy lenses representing the lower Pliocene continental-marine and meandering river plain facies. The aquifer base (1.4 Ma) consists of Pliocene marine deposits.

The occurrence of lowland springs (called "Fontanili" – Figs. 1 and 2) is observed across the entire Po Plain (E–W for about 800 km) in a 20-km-wide belt. These springs of phreatic water have been explained by the changes (from N to S) in both the ground surface slope gradient and the sediment grain size between the coarse-grained deposits of the high plain and finer deposits of the low plain (De Luca et al., 2014).

2.3. Low enthalpy geothermal exploitation in the study area

In 2019 the total number of installed GCHPs in the study area was 1,166 (2,321 boreholes in total) with a total power of 42 and 33 MW for heating and cooling, respectively. The mean power for a single system is about 40 kW for heating and 43 kW for cooling, and the average borehole length is about 105 m, ranging from 28 to 200 m (Fig. 3). These data were collected from the regional closed-loop system database active since 2006 (geothermal systems before that period are not included in this analysis) (Regione Lombardia, 2019a).

On the other hand, information about GWHPs are sparse and incomplete due to the fragmentation of local environmental management authorities. In this work we report only the 893 geothermal wells installed in the Milan metropolitan area (Città Metropolitana di Milano, 2019) that extract water from the shallow aquifer (aquifer "A" in Section 2.2).

Even if the datasets are not comparable, we can observe (Fig. 1) that open-loop systems tend to concentrate within the Milan city area where large power systems are more frequently installed. In fact, this solution is generally more attractive (and sometimes the only feasible after a cost-benefit analysis) for large systems due to the higher costs of installation and maintenance. On the other hand, closed-loop systems are typically installed for smaller power solutions such as residential buildings. For this reason, in the northern portion of the study area, where the population density is higher with respect to the southern part, the number of GCHPs is higher.

3. Materials and methods

The spatial distribution of thermal and hydrogeological parameters is essential to assess the potential of shallow geothermal systems. Depending on the adopted technology, i.e. GCHP or GWHP, the geothermal potential was obtained by means of different analytical methods.

For GCHP systems we implemented the ASHRAE (Kavanaugh and Rafferty, 2014) analytical equation for ground heat exchanger borehole length sizing. This method is based on the principle that the heat transfer rate to/from the ground is directly proportional to the borehole length and the temperature drop, and it is inversely proportional to the overall resistance of the ground and borehole materials.

Assuming that the heating load is equal to the cooling load, the thermal potential of closed-loop systems is given by the following equation (a detailed description of the terms of the equation is provided in the supplementary materials and Table 2):

$$P_{GSHP} = \frac{(t_g - t_f) + t_p}{q_a * R_{ga} + \frac{G}{Q} * (R_b + PLF * R_{gm} + F_{sc} * R_{gd})} \quad (1)$$

where

q_a is the net annual heat transfer rate from/to the ground obtained by considering the equivalent full-load hours (EFLH) for heating and cooling operating mode.

$$q_a = \frac{\left(1 - \frac{1}{COP_H}\right) * EFLH_H - \left(1 + \frac{1}{COP_C}\right) * EFLH_C}{8760} \quad (2)$$

R_b thermal resistance of the borehole lining and grout (mK/W)

PLF part-load factor (0.3 for common working time)

F_{sc} short-circuit heat loss factor between extraction and reinjection wells

t_g undisturbed ground temperature (°C)

t_f average temperature between the carrier fluid entering and leaving the heat pump (°C)

t_p long-term ground temperature penalty caused by ground heat

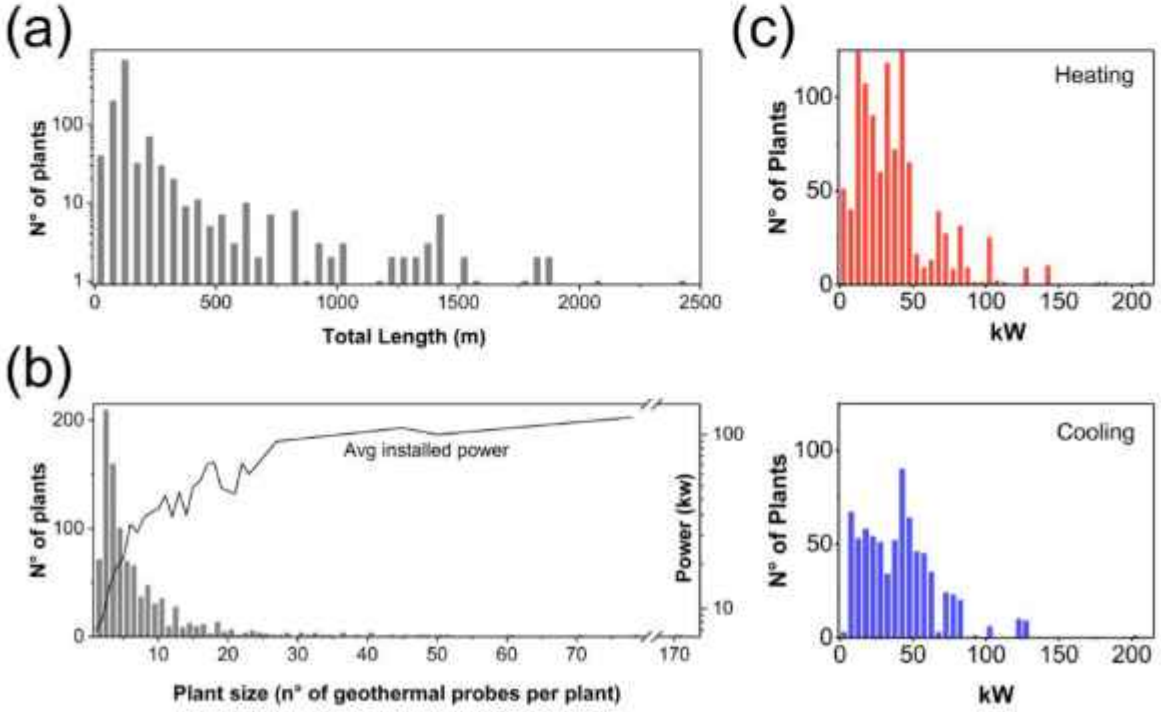

Fig. 3. Statistics of the installed closed-loop systems in the study area as on 2019: (a) amount of systems per length class, (b) amount of systems per size class versus the average installed power, (c) amount of systems per power class for heating and cooling modality.

transfer imbalances (°C)

R_{ps} R_{gm} R_{pt} equivalent thermal resistance of the ground to long-term, monthly and short-term heat pulses obtained through the Carslaw and Jaeger cylindrical heat source solution modified to account for time-varying heat pulses (Kavanaugh and Rafferty, 2014)

If we assume no significant imbalance between heating and cooling operating hours (i.e. the amount of heat extracted from the ground during the heating season is equal to heat injected into the ground during the cooling season, $t_p = 0$) Eq. (1) can be rewritten in a simplified (non-dominant) form:

$$P_{GCHP} = \frac{(t_g - t_f)}{\frac{G}{Q}(R_b + PLF * R_{gm} + F_{sc} * R_{ps})} \quad (3)$$

where the term G/Q is equal to (1-1/COP_H) in the heating mode and (1 + 1/COP_C) in the cooling mode, respectively. Thus, by fixing the system fluid temperature (tf), the duration of the heat pulses, and the correction factors (F_{sc}, PLF), P_{GCHP} depends essentially on the ground/groundwater temperature and the thermal diffusivity of the ground.

While closed-loop dimensioning is generally performed with standardized techniques, the open-loop thermal potential mostly depends on the hydrodynamic parameters of the aquifer and the thermal diffusivity is less relevant. In fact, the heat exchange potential of a GWHP system is strictly correlated to the amount of water withdrawable from the aquifer, according to hydrogeological and regulatory constraints.

The relation adopted to estimate the open-loop thermal potential depends on how much heat can be exchanged by a given water volume that passes through the heat exchanger and is expressed as follow:

$$P_{GWHP} = c_w \rho_w \, Q \, \Delta T \quad (4)$$

where

$c_w \rho_w$ Specific volumetric heat capacity of water (= 4.18 MJ/m^{3}K)

Q Flow rate (m^3/s)

ΔT Temperature difference between abstraction and injection wells (K).

Thus, P_{GWHP} depends essentially on the aquifer exploitability, i.e. on the transmissivity, on the existing regulatory thresholds about the abstraction and reinjection of water, and on the allowable thermal perturbation.

3.1. Data collection

The thermal potential of GCHPs and GWHPs depends on continuous variables (Eqs. (1) and (4)) that can be easily mapped for the entire study area through the interpolation of point information. The regional stratigraphic database (Regione Lombardia - CASPITA, 2019) collects the borehole logs available for the Lombardy-Po Plain area. The database contains information regarding the position, the elevation, the depth and the lithological description of the layers crossed by each borehole. In this study 8,854 logs were collected and stored in a georeferenced database. Then, by adopting the hierarchical classification of lithofacies and hydrofacies (De Caro et al., 2020), hydraulic and thermal parameters (Table 1) were assigned to each lithofacies as follows.

- **Hydraulic conductivity and porosity**: for the unconfined aquifer were assigned to each lithofacies unit by analyzing the grain size distribution and by adopting various empirical correlations between specific grain size curve coefficients and the equivalent hydraulic parameters (De Caro et al., 2020). Hydraulic parameters of the semi-confined aquifer units were assigned from the analysis of pumping test data provided by the local water supply agency (De Caro et al., 2020).
- **Thermal conductivity and specific volumetric heat capacity**: were assigned from the literature (Di Sipio et al., 2014; VDI 4640, 2001) to each single grain size unit (i.e. gravel, sand, silt and clay). The equivalent thermal parameters of composed units were obtained by the weighted average of each grain-size unit component according to its relative weight proportion. The relative proportions were assigned according to the Italian soil classification standard commonly used in borehole stratigraphic logging descriptions (A.G.I., 1963). In particular, in a multiple term unit, the first term represents the most abundant grain size class, then specific forms are used to distinguish if the abundance of additional terms ranges between 50 % and 25 %, 25 % and 10 % or 10 % and 5 % of the total weight.

The adopted hydrostratigraphic conceptual model (Fig. 2) is fully explained in De Caro et al. (2020), and will no longer be discussed in this work. The boundary surface between the phreatic and the semi-confined aquifer and the bottom boundary surface of the semi-confined aquifer were obtained from De Caro (2018). Piezometric head levels of the entire study area, as well as the digital elevation model (DEM cell size 5 × 5 m), were obtained from the regional geological database (Regione Lombardia, 2019b).

Table 1
Hydraulic and thermal parameters assigned to each lithofacies unit. K hydraulic conductivity, λ thermal conductivity for dry and wet soils, SVC specific volumetric heat capacity for dry and wet soils. Codification: G = Gravel, S = Sand, M = Silt, C = Clay, Cg = Conglomerate, Ss = Sandstone and P = Peat.

Aquifer	Gravel-Sandy Aquifers				Sandy-Gravel Aquifers						Soft-Rock Local Aquifers		
Hydrofacies	G	GS			GC	GM	S	SG		SM	R		
Lithofacies	*G*	*GS*	*GSC*	*GSM*	*GC*	*GM*	*S*	*SG*	*SGC*	*SGM*	*Ss*	*Cg*	*Rock*
K (m/s)	9.12 E-02	2.40 E-03	1.20 E-03	1.51 E-05	6.61 E-04	6.17 E-04	5.89 E-05	5.5 E-04	2.82 E-04	9.77 E-06	3.63 E-04	2.34 E-02	1.00 E-05

Aquifer	Aquitard / Deep Aquifers									Aquiclude				
Hydrofacies	M				SC		SM			C				
Lithofacies	*M*	*MC*	*MG*	*MS*	*SC*	*SCG*	*SM*	*SMC*	*SMG*	*C*	*CM*	*CG*	*CS*	*CP*
K (m/s)	9.55 E-06	6.13 E-06	6.92 E-06	5.62 E-06	1.10 E-05	1.62 E-05	2.19 E-05	4.27 E-06	5.89 E-06	5.50 E-09	1.23 E-07	3.47 E-06	5.50 E-06	8.13 E-06

Lithofacies	λ_{dry} (W/mK)	λ_{wet} (W/mK)	SVC_{dry} (MJ/m^{3}K)	SVC_{wet} (MJ/m^{3}K)
G	0.4	1.8	1.5	2.4
S	0.4	2.4	1.45	2.55
M	0.5	1.7	1.55	2.5
C	0.5	1.7	1.55	2.5
Cg	2	2	2	2
Rock	2.3	2.3	2.2	2.2

3.1.1. Thermal and hydraulic parameters

Equivalent thermal parameters were obtained for four reference borehole length scenarios (50, 100, 150 and 200 m below the ground surface) by computing the weighted average of each unit along the borehole and by taking into account the presence of water (Fig. 4). For each depth scenario only the stratigraphic logs reaching the reference length (with a 20 % tolerance) were selected. The number of boreholes used to interpolate the parameters in each scenario was: 4693, 2988, 1302 and 627 respectively for the 50, 100, 150 and 200 m reference depth intervals.

Then, by interpolating via ordinary kriging the equivalent thermal parameters of each borehole we obtained the thermal conductivity and volumetric heat capacity maps for each depth scenario (e.g. Fig. 5a and b show the equivalent values for the 100 m reference borehole length).

The equivalent horizontal hydraulic conductivity was calculated at each borehole location only for the unconfined aquifer (Fig. 4) and, by multiplying by the saturated thickness (which is generally lower than 100 m), the transmissivity of the phreatic aquifer (Fig. 5c and d) was obtained.

The areas considered for the thermal (Fig. 5a and b) and hydraulic parameters (Fig. 5c and d) differ in extent because to the north of the dashed line ("aquitard boundary") the shallow phreatic aquifer is not fully separated from the deeper aquifers (as evidenced also by the cross-section in Fig. 2). Thus, the regionalization of the aquifer transmissivity values is not applied because the thickness and the extension (but also the hydraulic properties) of the shallow aquifer vary significantly at local-scale, and the aquifer parameters cannot be related to those south of the "aquitard boundary" line.

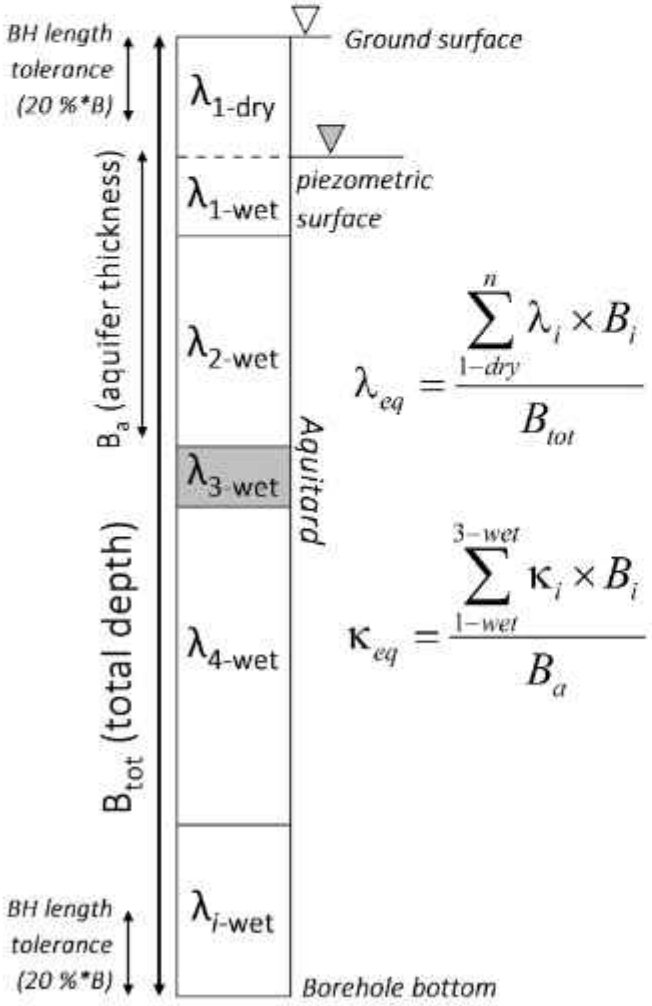

Fig. 4. Schematic representation of the procedure for the calculation of equivalent thermal and hydraulic parameters.

3.1.2. Groundwater temperature

The underground temperature is one of the most difficult parameters to assess in regional-scale geothermal potential studies since it is controlled by various local-scale phenomena, such as (I) the thickness of the unsaturated zone that dampens the temperature fluctuations coming from the surface, (II) the groundwater flow velocity that drives the heat transport in advective-dominated aquifers, (III) the presence of surface water bodies and the degree of interaction with the groundwater, (IV) the percentage of sealed/cemented ground, (V) the presence of underground structures/infrastructures (e.g. tunnels) or deep foundations and (VI) the use of low-enthalpy geothermal wells (Epting and Huggenberger, 2013; Kurylyk et al., 2015).

In regional scale geothermal potential studies some authors considered the mean annual underground temperature equal to the mean annual air temperature (Viesi et al., 2018), while others related the underground temperature to other variables such as the altitude or the latitude (Galgaro et al., 2015; Perego et al., 2019; Signorelli and Kohl, 2004).

Since in the study area only 32 air temperature monitoring stations are available (Fig. 6a), we collected water temperature data from physic-chemical datasets provided by local and regional water supply agencies, from Thermal Response Tests values reported in the regional closed-loop system database (Regione Lombardia, 2019a) and from multi-temporal vertical temperature profiles collected for the shallow aquifer with a multi-meter probe. After homogenization and quality check (only those points with at least four measurements at different times of the year were considered) the datasets were merged into a single spatial database to obtain the mean annual groundwater temperature. 750 temperature data representative of the phreatic and the semi-confined shallow aquifers were used and interpolated in the study area through ordinary kriging (Fig. 6b). The mean annual air temperature and the mean annual temperature of the shallow groundwater are well correlated in the study area (Fig. 6c and d). The most relevant deviation is observed in the northern portion of the study area and downwards the Milan city area. In the first case, the groundwater temperature is lower than the air temperature due to the greater depth of the water table whereas, in the second case, the groundwater temperature is higher due to the propagation of the heat island effect towards the main flow direction (i.e. parallel to the section line A-A' in Fig. 6B).

3.1.3. Climatic data

The amount of thermal energy required to heat/cool indoor spaces depends on the external air temperature and the thermal insulation characteristics of each building. In this study we collected mean hourly air temperature data from 69 rain gauge stations (32 inside the study area) available for the last three years (2017–2019).

One of the most common simplified methods to estimate building energy consumption is to derive the equivalent full-load operating hours (EFLH) from climatic data. The EFLHs describe the number of hours a cooling or heating system needs to operate at full load to consume the total annual required amount of energy as expressed by the following equation:

$$EFLH = \frac{\sum hDDs}{|T_{peak} - T_{ref}|} \quad (5)$$

where

hDDs are the hourly degree days obtained as the difference between the mean hourly air temperature and the reference indoor temperature (T_{ref}) for cooling mode and, vice versa, for heating mode. According to Banks (2009a) T_{ref} was set to 18.3 °C for heating and 23.8° for cooling, respectively;

T_{peak} is the project peak temperature and was assumed as the 1st and

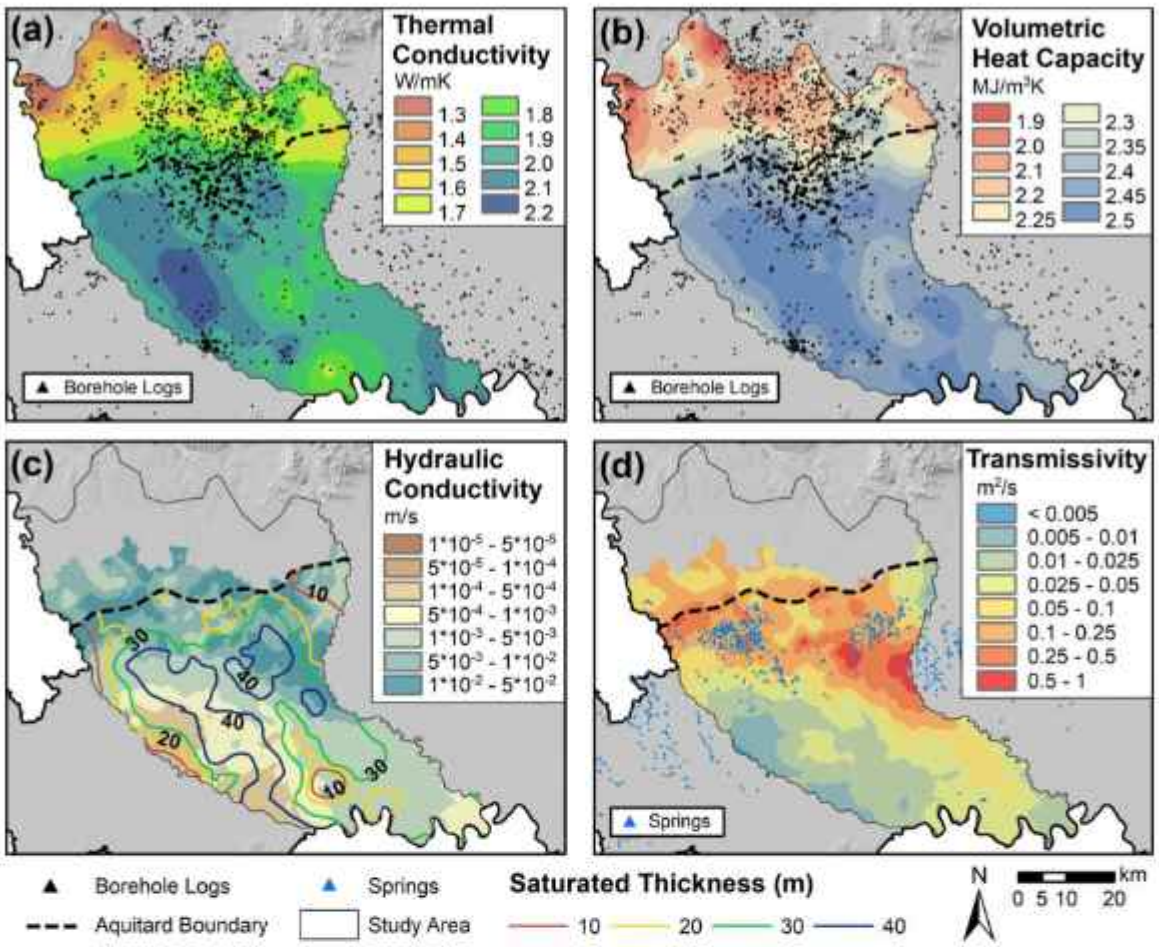

Fig. 5. Maps of the study area showing: (a) the equivalent thermal conductivity and (b) the equivalent volumetric heat capacity for the 100 m reference length scenario, (c) the equivalent horizontal hydraulic conductivity, the saturated thickness and (d) the transmissivity of the phreatic aquifer.

the 99th percentiles of the mean hourly air temperature frequency cumulative distribution for heating and cooling mode, respectively (ASHRAE, 2009).

To obtain the annual EFLH, the sum (considering only positive values) of the hourly degree days over an entire year (8760 h in total) was divided by $T_{peak} - T_{ref}$.

Fig. 7 shows the spatial distribution of the EFLHs obtained for heating and cooling. We can observe that, due to the heat island effect, in the Milan city area the number of EFLHs for cooling is higher than anywhere else in the study area and, conversely, the number of EFLHs for heating is the lowest.

4. Closed-loop geothermal potential

Since GCHPs do not require the abstraction of groundwater and the main limiting factor is the techno-economic feasibility, the spatial distribution of the technical thermal potential is pivotal to their development. Some restrictions to the installation of GCHPs exist if there is the possibility to connect the aquifers exploited for drinking water withdrawal with more contaminated shallow aquifers (Busby et al., 2009). This can be prevented by a properly grouted section along the aquitard that also provides a good thermal contact if a high thermal conductivity grout is used. According to the regional geothermal regulation (Regione Lombardia, 2010), the installation of a GCHP system in the study area is allowed without restrictions up to 150 m in depth while deeper installations are subjected to an authorization procedure and the assessment of the thermal impact of the system is required. Furthermore, for the installation of GCHPs with a thermal power greater than 50 kW the Thermal Response Test is also required.

According to the regional closed-loop system database (Fig. 3), a length of 100 m was considered as the most likely exploitation scenario. The thermal potential was calculated in non-dominant mode (Eq. (3)), i.e. by assuming no imbalance between cooling and heating loads and no significant differences between the amount of heat extracted from the ground during the heating season and the heat injected into the ground during the cooling season. Then, the result was compared with the thermally unbalanced potential obtained by means of Eq. (1) considering 50 years' lifetime and the operative equivalent full-load hours for heating and cooling as described above. The parameters adopted in Eq. (1) and (3) are listed in Table 2.

Fig. 8 shows the closed-loop geothermal potential for a 100-meters-length GCHP. Non-dominant thermal potential ranges between 35 and 67 W/m of installed borehole but, considering the operative EFLHs (Fig. 7) it can decrease up to 12 % and increase up to 16 % for heating and cooling mode, respectively. We can observe that GCHPs are more efficient in the southern portion of the study area where the water table is closer to the surface. To the north we can observe greater potential values in the eastern sector due to the presence of shallower conglomeratic units (e.g. the "Ceppo" formation), that are generally more conductive than loose deposits. The thermal potential in the Milan city area decreases significantly switching from heating to cooling modality as a result of the heat island effect.

5. Open-loop geothermal potential

The open-loop geothermal potential depends essentially on the

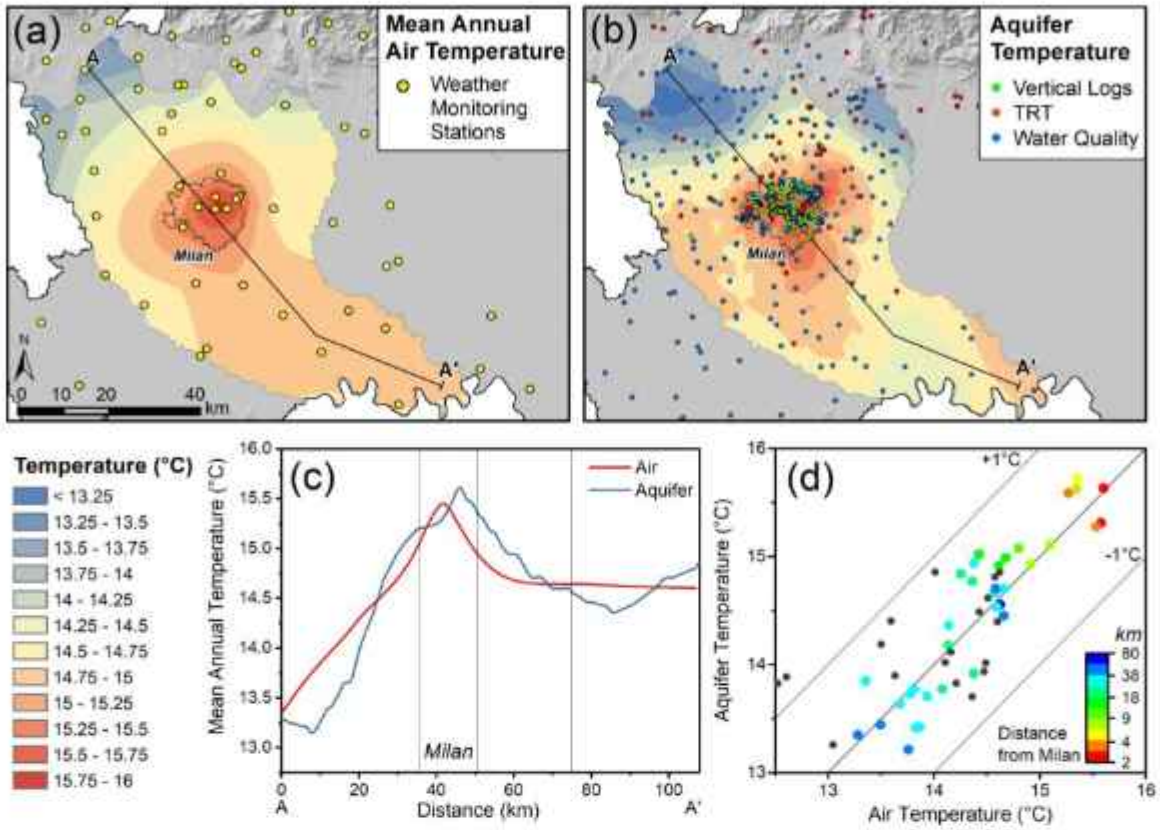

Fig. 6. (a, b) Maps showing the spatial distribution of the mean annual air and aquifer temperature, respectively. (c) Mean annual air and aquifer temperature along the AA' profile and (d) scatter plot showing the correlation between the mean annual aquifer temperature and the mean annual air temperature. Dots are colored by the distance from the Milan city area, where the highest temperature is observed.

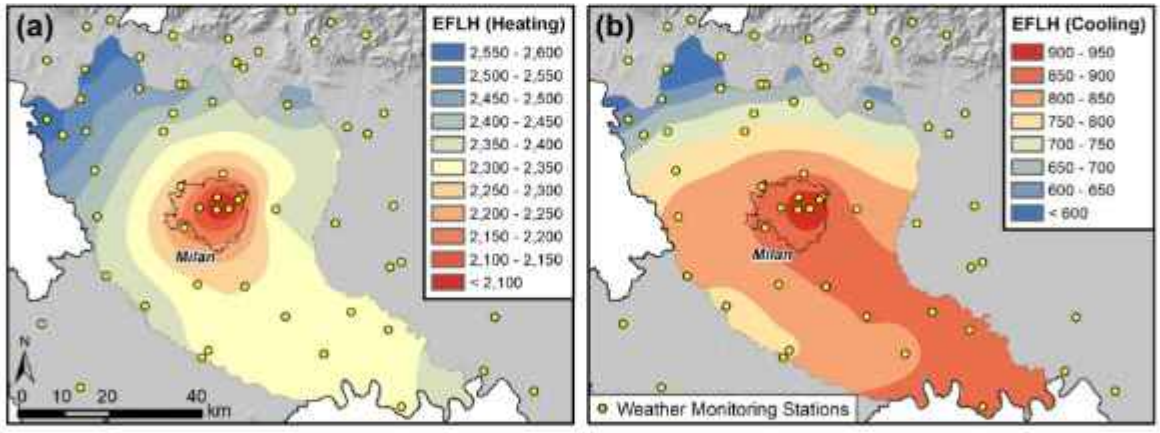

Fig. 7. Maps showing the spatial distribution of the annual equivalent full-load hours (Eq. (5)) for heating (a) and cooling (b).

amount of water that can be extracted and re-injected from/into the aquifer or disposed in a surface water body. This amount depends firstly on the aquifer characteristics, such as the transmissivity, but also on the regulations about the use and the conservation of the quantity and the quality of the groundwater resources. Following the steps proposed by Böttcher et al. (2019), we adopted the following thresholds based on local regulatory restrictions and common groundwater conservation principles:

1 **Maximum recommended drawdown** (Q_d): was imposed to avoid excessive consumption of the groundwater resources. According to Bezelgues-courtade et al. (2010) well dynamic piezometric level should not be lower than one-third of the saturated thickness of the phreatic aquifer and the drawdown must not exceed a threshold value. Drawdown thresholds are also important to prevent soil settlements in urban areas. For this reason, in addition to the one-third rule we set a maximum well lowering threshold of 10 m. This value represents the mean historical groundwater level recorded in the Milan city during the' 70 s due to the remarkable depression cone caused by intensive groundwater withdrawals (Crosta and De Caro, 2018). If the shallow deposits in the Milan city area have undergone consolidation due to the pore pressure lowering in the past decades, the surrounding less urbanized areas have not experienced such a phenomenon. For this reason, the 10-meters-threshold must be cross-checked with site-specific assessments in the areas where the difference between the present and the historical groundwater levels

Table 2
Overview of the parameters used for the calculation of GCHP thermal potential.

Parameter		Description	Unit	Value
t_z		Undisturbed ground temperature	°C	**Raster map** (Fig. 6b)
t_f		Temperature threshold of the carrier fluid	°C	−2 (heating), 32.5 (cooling)
t_p		Temperature penalty resulting from imbalances between the heat removed and injected in heating and cooling mode ($EFLH_H/EFLH_C > 2$)	°C	−0.5
$EFLH_H$ $EFLH_C$		Equivalent full-load hours	h	**Raster map** (Fig. 7)
R_b		Borehole thermal resistance	mK/W	↓
	λ_{gr}	Thermal conductivity of the grout	W/mK	2
	d_b	Borehole external diameter	m	0.075
	d_p	Pipes diameter	m	0.016
	n	Number of pipes	–	4
PLF		Part-load factor according to (Kavanaugh and Rafferty, 2014)	–	0.9
F_{sc}		Short circuit heat loss factor (one U-tube in series, $q_{carrier\_fluid} = 0{,}05\ l/s\,kW$)	–	1.05
R_{ga} R_{gm} R_{gst}		Thermal resistance of the ground calculated for the long-term (a), monthly (m) and short-term (st) heat pulses	mK/W	↓
	λ_g	Equivalent thermal conductivity of the ground	W/mK	**Raster map** (Fig. 5a)
	$c_g\rho_g$	Equivalent volumetric heat capacity	J/m³K	**Raster map** (Fig. 5b)

is significantly lower than 10 m. Those areas are pointed out in Fig. 10.

2 **Maximum allowable rising** (Q_r): was imposed to avoid an excessive rise of the groundwater level that might result in basements or surface flooding. According to typical underground basement depths, the level of the groundwater should not overcome at least three meters below the ground surface. In some portions of the study area, the water table is so close to the surface (less than 2 m) that the re-injection of water must be carefully planned. If the disposal in surface water bodies is not achievable some "low-impact" re-injection techniques can be adopted such as a group of reinjection wells instead of a single well or drainage trenches.

The maximum flow rate to avoid excessive rising and drawdown was derived through the Cooper & Jacob equation:

$$Q = \frac{4\,\pi\,T\,\Delta H}{\log(2{,}25\frac{T\,t_{pump}}{s\,r_w^2})} \quad (6)$$

3 **Thermal breakthrough constraint** (Q_b): the reinjection of water downstream or upstream to the abstraction well causes a thermal alteration plume. Not properly sized geothermal well fields can undergo thermal recycling processes if the thermal alteration plume propagates back towards the abstraction well, reducing the efficiency of the system (Banks, 2009b). Depending on the discharge of the system, the minimum injection/extraction well distance can be estimated according to Eq. (7) (Banks, 2009b; Lippman, 1980). By setting the reference space length to a typical value (according to (Regione Lombardia, 2019a) L = 100 m) we can obtain the maximum allowable flow rate to prevent the thermal breakthrough between a 100-meters-spaced well doublet:

$$Q = \frac{\pi * L * T * i}{1{,}96} \quad (7)$$

4 **Temperature difference constraint:** according to the local regulation on the use of shallow groundwater resources (Regione Lombardia, 2017) the maximum temperature change between the abstraction and injection wells was set to 5 °C. Moreover, the maximum reinjection temperature is restricted to 21 °C.

Fig. 9 shows the maximum recommended flow rate according to the drawdown and rising constraints and the relative minimum distance between the extraction and injection well obtained by substituting the maximum flow rate in Eq. (7). The area considered for the installation of GWHPs (Figs. 9 and 11) differs in extent from that of GCHPs (Fig. 8) as explained in Section 3.1.1. The installation of GWHPs north of the dashed line is still possible but to assess the thermal potential local investigations are necessary.

The Milan metropolitan area is the most urbanized portion of the study area. In this region many industrial activities have flourished since the early 60 s leading to intense groundwater exploitation up to the early 90 s. If during the industrial period the water table was lowered by up to more than 15 m, nowadays most of the activities have been relocated and the groundwater rebound phenomenon has been observed in many piezometric time series (Crosta and De Caro, 2018). By comparing the historical piezometric data available for the study area we estimated the maximum groundwater fluctuation as the difference between the present level and the lowest recorded historical level (Fig. 10). Where the historical groundwater fluctuations are lower than 10 m we suggest considering if soil settlements caused by the lowering of the groundwater table can damage surface infrastructures.

The effective open-loop geothermal potential (P_{GWHP} [W]) was derived by combining the maximum flow rate obtained from Eqs. (6) and (7) considering two operative configurations:

- Re-injection of wastewater: $P_{GWHP} = c_w\rho_w\,\Delta T\,min(Q_d, Q_r, Q_b)$ (8)
- Surface disposal: $P_{GWHP} = c_w\rho_w\,\Delta T\,Q_d$ (9)

The parameters adopted in Eq. 6, 7, 8 and 9 are summarized in Table 3.

The open-loop geothermal potential (with and without reinjection) is presented in Fig. 11. We can observe that to the south of the lowland spring belt, due to the proximity of the water table to the surface, the thermal potential is strongly limited by the groundwater rising constraint and, generally, the thermal potential is higher if only the abstraction of groundwater is considered. The disposal of wastewaters in surface water bodies (e.g. canals, rivers, lakes) is possible if they border (or flow very close to) the installation site property boundaries, which is unlikely in urban areas and frequently restricted. Nevertheless, the Milan area is characterized by the presence of a dense network of channels (Navigli) and others of minor order (see Fig. 1) that could constitute in specific cases a way of disposing the thermally altered wastewaters.

6. Discussion

A regional geothermal potential mapping aims to promote sustainable planning and design of shallow geothermal systems such as GCHPs and GWHPs. In this work we assessed the capability of the study area to host different low enthalpy geothermal systems. Therefore, under different assumptions, specific heat exchange rates were derived by combining the spatial distribution of hydraulic and thermal parameters of the underground and the aquifer characteristics (e.g. the transmissivity) with the groundwater temperature and some regulatory restrictions.

During the last years in Europe many efforts were made to derive the geothermal potential in densely populated areas such as the metropolitan area of Barcelona (García-Gil et al., 2015), the city of Basel (Epting et al., 2018) and Munich (Böttcher et al., 2019), in Alpine regions

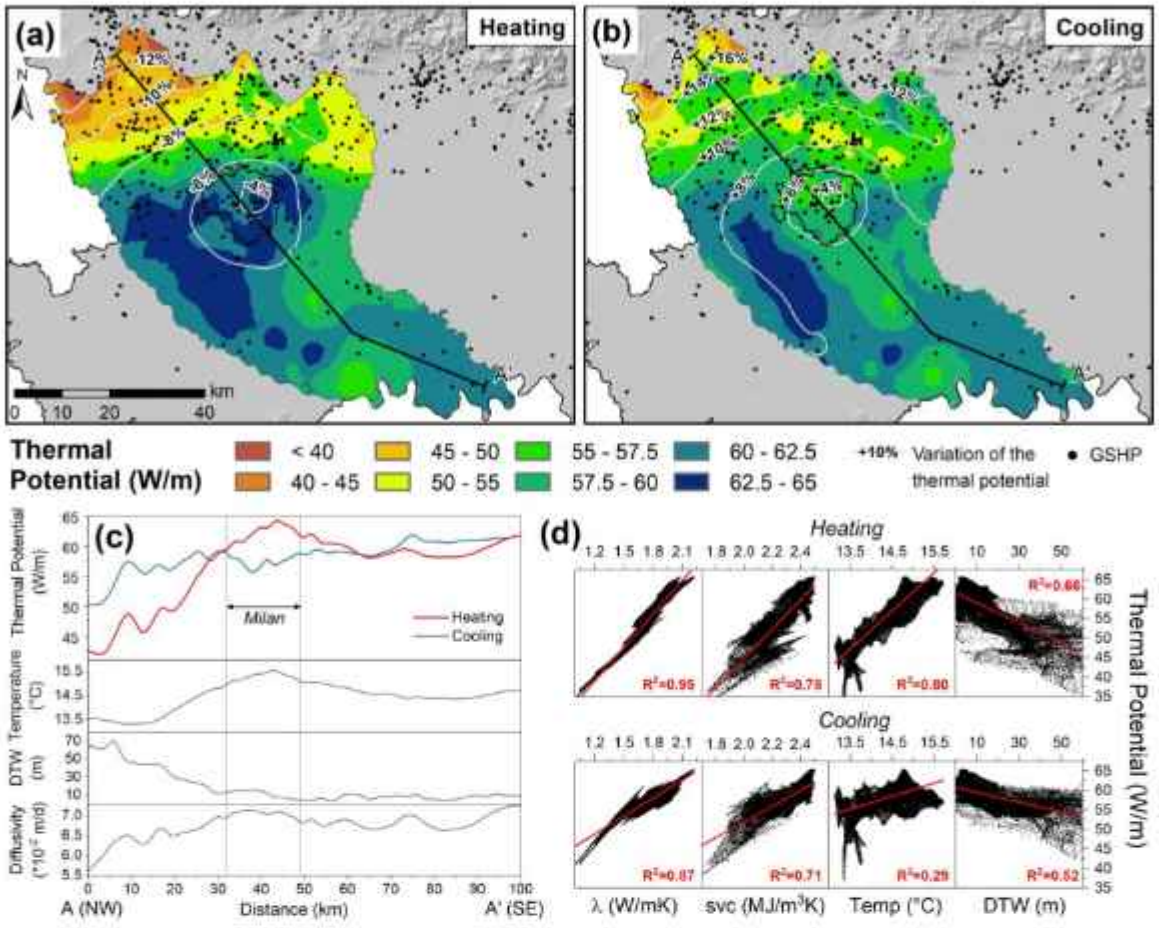

Fig. 8. (a, b) Maps showing the spatial distribution of the GCHPs (non-dominant, Eq. (3)) thermal potential for heating and cooling mode, respectively. Grey isolines represent the increase/reduction of the thermal potential if the general equation is considered (Eq. (1)) instead of the non-dominant form. (c) Cross-section profiles and (d) correlation between the thermal potential and the thermal parameters (λ and svc), the groundwater temperature and the depth of the water table (DTW).

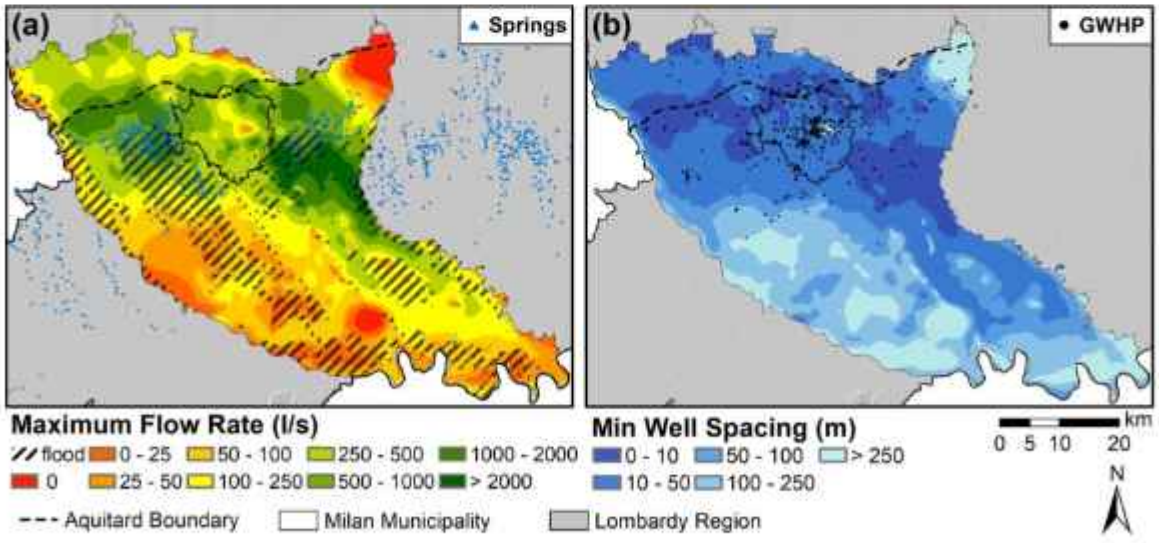

Fig. 9. (a) Maximum recommended flow rate obtained by combining the drawdown and rising constraints and (b) minimum allowable distance to prevent thermal breakthrough between the extraction and the injection well. Banded field ("flood") represents the area where re-injection of wastewater is not allowed to avoid basement flooding.

(Casasso et al., 2017; Casasso and Sethi, 2016; Viesi et al., 2018) but also at the scale of entire Europe (Bertermann et al., 2015). Generally, the main challenge is to obtain the effective potential basing on underground data and real operative conditions (i.e. the "technical potential" (Bayer et al., 2019)). This issue is well addressed in the work by analyzing and merging different datasets (e.g. stratigraphic information,

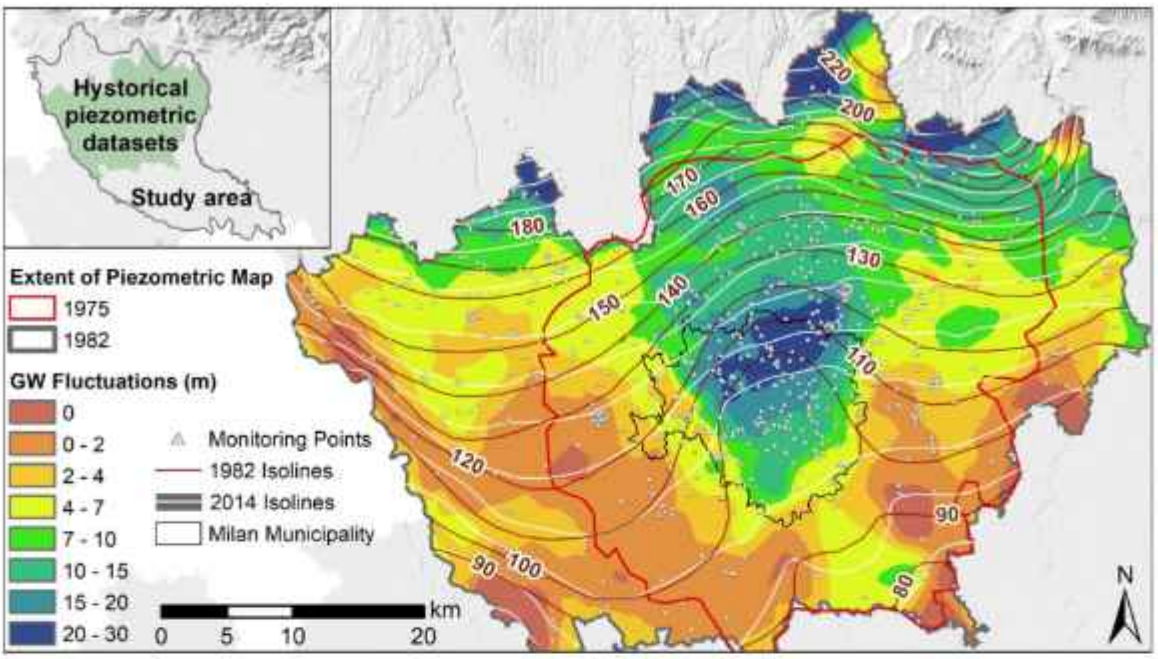

Fig. 10. Map of the Milan Metropolitan Area showing the spatial distribution of the difference between the minimum historical piezometric level and the piezometric level as on 2016. Piezometric levels within the red area were obtained from the piezometric map available for 1975, whereas outside this area a piezometric map of 1982 and piezometric point data were compared (For interpretation of the references to colour in this figure legend, the reader is referred to the web version of this article).

Table 3
Overview of the parameters used to derive the thermal potential of GWHPs.

Parameter		Description	Unit	Value
T		Transmissivity of the shallow aquifer	m^2/s	**Raster map** (Fig. 5d)
B		Saturated thickness of the shallow aquifer	m	**Raster map** (Fig. 5d)
ΔH	Abstraction	Max. allowable drawdown	m	$min\left(\frac{1}{3}B; 10\ m\right)$
	Injection	Max. allowable rising	m	$s - h < 3$ m
L		Distance between abstraction and injection wells	m	100
t_{pump}		Pumping time (180 days/year for 50 years)	s	$7.9*10^8$
r_w		Well radius	m	0.25
S		Storage coefficient	[]	0.2
$c_w\rho_w$		Volumetric heat capacity of water	J/m^3K	$4.18*10^6$
ΔT		Regulatory threshold on temperature perturbation	°C	5

groundwater temperature data and climatic conditions). The results obtained in this study are consistent with those obtained from various studies in other European cities and demonstrate the high potential of a highly conductive alluvial aquifer, especially if the thermal energy demand is very high.

Nevertheless, the outcome of this work should not be considered as a specific design rule for the installation of geothermal systems but could be significant for regional energy planning and stakeholders. The thermal potential maps are therefore the preliminary step for further local assessments and in-situ efficiency tests that better characterize the effective heat exchange rate under real design conditions.

6.1. Comparison with other methods

A general assessment of the low enthalpy geothermal potential in this area was provided by the local environmental authority (Regione Lombardia, 2019c) for the only closed-loop configuration. This evaluation is based on the juxtaposition of specific extraction rates provided by the German guidelines (VDI 4640, 2001) on the spatial distribution of shallow loose deposits and outcrops derived from the regional scale geological map. The German guidelines are based on empirical correlations between real extraction rates and lithologies at the development sites and are commonly adopted by GCHP installers as a "rule of thumb" but have some limitations. Firstly, the ground and groundwater temperature that affects the efficiency of the system are not considered. Moreover, there is no distinction between heating and cooling mode and the real operating hours per year are not considered. Lastly, the existing potential map is based only on the shallow deposits and outcrops whereas also the vertical variability should be considered to predict the overall thermal response of deep borehole heat exchangers. In this study we overcome these limitations by integrating hydraulic and thermal parameters and temperature data into the analytical equation proposed by Kavanaugh and Rafferty (2014).

As regards the open-loop configuration there are no thermal potential studies in this area due to the highly fragmented regulation on the use of groundwater for thermal purposes. The authors think that this lack has strongly hindered the development of this technology in the study area.

6.2. Considerations on the use of GCHP or GWHP

The best choice between GCHPs and GWHPs, from an energy-efficiency and economical point of view, may depend on several aspects, among these: [1] the possibility to withdraw/reinject water from/into the aquifers; [2] the space availability to place the extraction and injection wells far enough to prevent thermal short-circuiting; [3] the prevention of local excessive groundwater fluctuations and soil subsidence that can damage structures and infrastructures (Stauffer et al., 2013). Apart from these technical limitations, one of the most important deciding factors is the required thermal load. Generally, for large plants it is preferable to decide for an open-loop system, whereas for smaller ones both solutions are suitable. This is due to the high transmissivity of the aquifers in the study area that can provide a wide range of flow rates

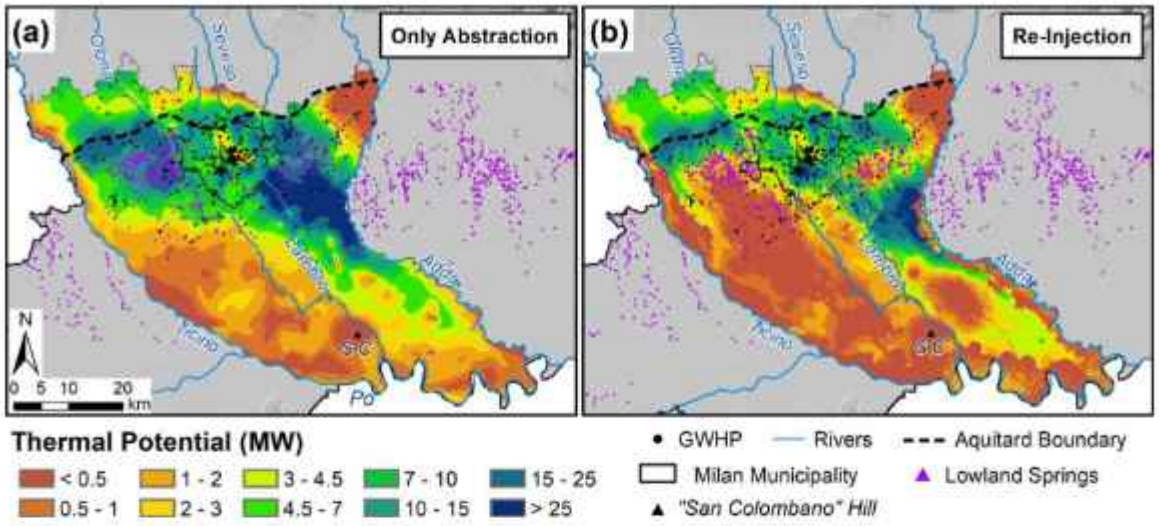

Fig. 11. Maps showing the spatial distribution of the GWHP thermal potential for the only-abstraction (a) and the re-injection operative mode (b).

for a single well (this rule could not be valid in different hydrogeological settings). On the contrary, the ratio between the thermal load and the required GCHP length is generally constant, leading to unprofitable drilling costs for great energy demand projects. In Fig. 12 the required GCHP length and the number of geothermal wells for two thermal load scenarios are compared. Fig. 12a shows the minimum length required by a GCHP system to satisfy a 45 kW thermal load, whereas Fig. 12b shows the number of geothermal wells required to satisfy a 10 MW thermal load assuming that each well is working at its highest flow rate potential. The contour lines in each representation display a comparison with the other methodology. We can observe that for a 45 kW thermal load the total GCHP length ranges between 750 and 1000 m (between 7 and 10 100-meters-length GCHPs) whereas the same load could be satisfied by a GWHP system using at most 1% of its maximum potential. On the contrary to fulfill a 10 MW heat demand up to 10 abstraction wells might be necessary for the study area. This great amount of energy could be satisfied with an estimated average number of about 2000 100-meters-length GCHPs. This solution is unrealistic or hardly feasible both for the required space and the total drilling costs. In fact, from a local cost analysis, considering about 50÷60 €/m for drilling and setting up a GCHP system, and 200÷300 €/m for a GWHP system, in the first scenario both technologies are profitable whereas in the second scenario the GCHP configuration is unprofitable.

6.3. Thermal potential and city-scale heat demand

The study area covers one of the most densely populated regions in Italy and Europe and this is reflected by an intense thermal energy demand for heating and cooling purposes. A countercheck of the potential of the study area to host shallow low-enthalpy geothermal systems was made by comparing the calculated thermal potential with the actual thermal energy demand based on the energy used in 2019 by conventional systems (e.g. gas/oil/coal burning systems, air-coupled heat pumps) in each municipality (Regione Lombardia, 2019d). The average actual thermal demand of each municipality was compared with the thermal potential of a 100-meters-length GCHP (Fig. 13a and b) whereas the maximum actual thermal demand was compared with the thermal potential of GWHPs systems (Fig. 13c and d).

We can observe that the average thermal demand in the study area can almost everywhere be satisfied by a number of GCHPs between 4 and 20 (Fig. 13b). This solution is attractive from an initial investment cost point of view and can be adopted in the whole study area without restrictions. The energy demand of big buildings or entire city districts (supplied by district-heating) is represented by the maximum thermal

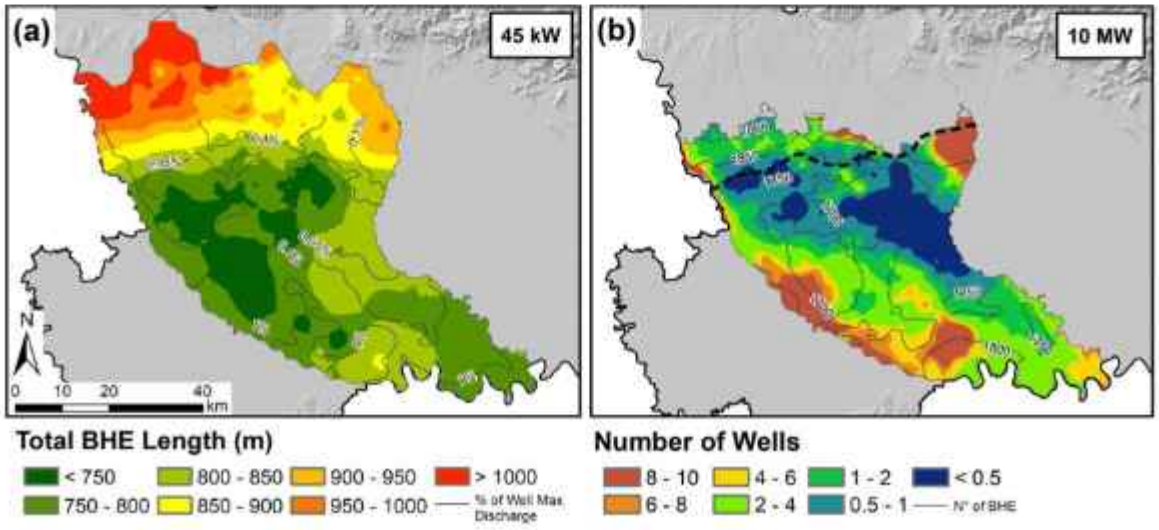

Fig. 12. (a) Map showing the spatial distribution of the length required by a GCHP system to fulfill a 45 kW thermal load and (b) map showing the spatial distribution of the number of wells required to meet a 10 MW thermal load. The two areas in the figure differ in extent as explained in Section 3.1.1.

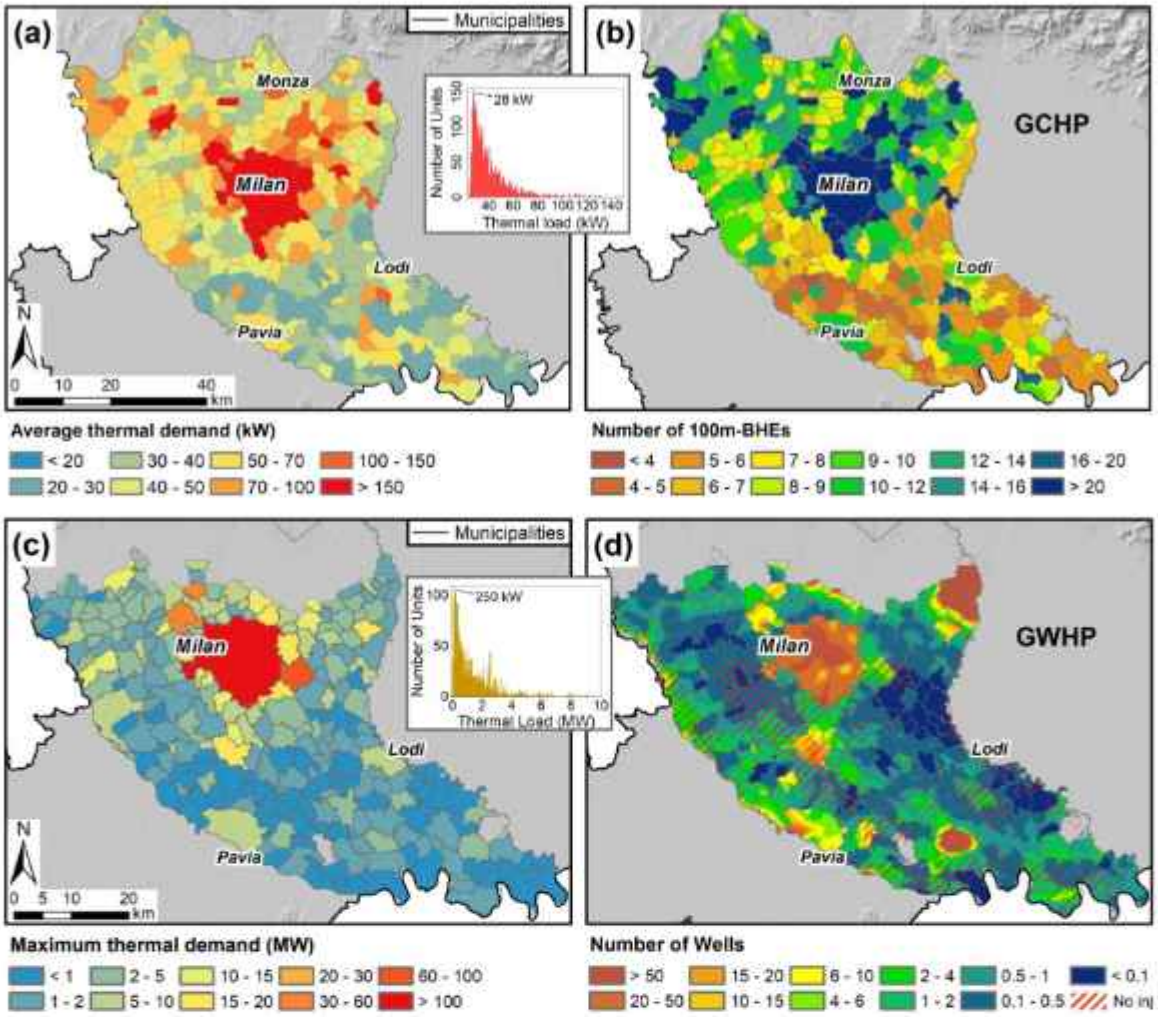

Fig. 13. Maps showing the spatial distribution of (a) the average thermal demand based on the energy used in 2019 by conventional systems in each municipality, (b) the number of 100-meters-length GCHPs required to satisfy the average thermal demand, (c) the maximum thermal demand of each municipality and (d) the number of geothermal wells required to satisfy the maximum thermal demand.

load and can be fulfilled by at most a group of 20 geothermal wells (Fig. 13d). However, for a large number of municipalities in the study area (except for the Milan city) the maximum thermal demand could be fulfilled by one or two wells.

7. Conclusions

A comprehensive regional assessment of the low enthalpy geothermal potential for both closed- and open-loop systems in a densely urbanized area is presented. The methodology proposed is based on the analysis of geological, hydrogeological and climatic components, and includes technical and legislative constraints, together with groundwater quantity and quality conservation principles.

The main factors which control the potential of GCHPs and GWHPs are the groundwater table depth, the transmissivity of the phreatic aquifer, the groundwater temperature and the thermal parameters of the aquifers. The effective thermal potential of closed-loop systems is calculated for both heating and cooling modes by combining the mean annual groundwater temperature derived from direct measurements with site-specific ground thermal parameters averaged on the entire length of the borehole. On the other hand, the open-loop thermal potential is based mostly on the productivity of the shallow aquifers by considering the effects of groundwater extraction and re-injection on the water table fluctuations to prevent excessive drawdown or rising, potential soil settlements and to avoid thermal short-circuit.

The depth to be drilled to fulfill a 45 kW thermal load with GCHPs ranges from 680 to 1200 m and from 720 to 1100 m for heating and cooling mode, respectively. In case of GWHPs the depth to be drilled is restricted to the depth of the bottom of the phreatic aquifer and ranges between 10 and 50 m. By considering specific discharge thresholds and temperature differences the thermal potential of GWHPs is obtained and compared with the thermal potential of GCHPs in the previous section. Where both solutions are possible from a technical point of view, this study could be improved by a long-term cost-benefit analysis to reveal which could be the less expensive solution.

With this study we demonstrated the high potential of the study area to host different kinds of low enthalpy geothermal systems by giving specific heat exchange rates with the ground/groundwater. The high thermal energy capacity of the area was confirmed by the possibility to fulfill the thermal energy used in 2019 by non-renewable systems in each municipality through the installation of GCHPs and GWHPs.

CRediT authorship contribution statement

Alberto Previati: Conceptualization, Methodology, Investigation, Data curation, Writing - original draft, Visualization. **Giovanni B. Crosta:** Conceptualization, Writing - review & editing, Supervision, Funding acquisition.

Declaration of Competing Interest

The authors declare that they have no known competing financial interests or personal relationships that could have appeared to influence the work reported in this paper.

Acknowledgments

The authors are grateful to Marta Gangemi and Fabio Marelli (MM S. p.a), Maurizio Gorla and Chiara Righetti (Gruppo CAP) for providing essential data and supporting the groundwater monitoring activities.

This article is an outcome of the Project PRIN MIUR Urgent - Urban geology and geohazards: Engineering geology for safer, resilient and smart cities, 2017 HPJLPW and, Project MIUR – Dipartimenti di Eccellenza 2018–2022 and PerFORM WATER 2030, Regione Lombardia project.

Appendix A. Supplementary data - ASHRAE method

Supplementary material related to this article can be found, in the online version, at doi:https://doi.org/10.1016/j.geothermics.2020.101999.

References

A.G.I, 1963. Nomenclatura geotecnica e classifica delle terre (Italian soil classification standard).

ASHRAE, 2009. Handbook HVAC Fundamentals. Ashrae.

Banks, D., 2009a. An introduction to thermogeology and the exploitation of ground source heat. Q. J. Eng. Geol. Hydrogeol. 42, 283–293.

Banks, D., 2009b. Thermogeological assessment of open-loop well-doublet schemes: a review and synthesis of analytical approaches. Hydrogeol. J. 17, 1149–1155. https://doi.org/10.1007/s10040-008-0427-6.

Bayer, P., Attard, G., Blum, P., Menberg, K., 2019. The geothermal potential of cities. Renew. Sustain. Energy Rev. 106, 17–30. https://doi.org/10.1016/J.RSER.2019.02.019.

Bertermann, D., Klug, H., Morper-Busch, L., 2015. A pan-European planning basis for estimating the very shallow geothermal energy potentials. Renew. Energy 75, 335–347. https://doi.org/10.1016/j.renene.2014.09.033.

Beseiglues-courtade, S., Martin, J., Schomburgk, S., Nguyen-the, D., Nguyen, D., Le Brun, M., Desplan, A., 2010. Geothermal Potential of Shallow Aquifers: Decision-Aid Tool for Heat-Pump Installation.

Blum, P., Campillo, G., Münch, W., Kölbel, T., 2010. CO2 savings of ground source heat pump systems - A regional analysis. Renew. Energy 35, 122–127. https://doi.org/10.1016/j.renene.2009.03.034.

Böttcher, F., Casasso, A., Götzl, G., Zosseder, K., 2019. TAP - Thermal aquifer Potential: a quantitative method to assess the spatial potential for the thermal use of groundwater. Renew. Energy 142, 85–95. https://doi.org/10.1016/j.renene.2019.04.086.

Busby, J., Lewis, M., Reeves, H., Lawley, R., 2009. Initial geological considerations before installing ground source heat pump systems. Q. J. Eng. Geol. Hydrogeol. 42, 295–306. https://doi.org/10.1144/1470-9236/08-092.

Casasso, A., Sethi, R., 2016. G.POT: a quantitative method for the assessment and mapping of the shallow geothermal potential. Energy 106, 765–773. https://doi.org/10.1016/j.energy.2016.03.091.

Casasso, A., Piga, B., Sethi, R., Prestor, J., Pestotnik, S., Bottig, M., Goetzl, G., Zambelli, P., D'Alonzo, V., Vaccaro, R., Capodaglio, P., Olmedo, M., Baietto, A., Maragna, C., Böttcher, F., Zoesseder, K., 2017. The GRETA project: the contribution of near-surface geothermal energy for the energetic self-sufficiency of Alpine regions. Acque Sotter. - Ital. J. Groundw. 6 https://doi.org/10.7343/as-2017-265.

Crosta, G.B., De Caro, M., 2018. Groundwater rebound. In: Bobrowsky, P., Marker, B. (Eds.), Encyclopedia of Engineering Geology. Springer International Publishing, Cham, pp. 1–3. https://doi.org/10.1007/978-3-319-12127-7_151-1.

De Caro, M., 2018. Analysis of Groundwater Environment Change in the Milan Metropolitan Area by Hydrostratigraphic, Groundwater Quality and Flow Modeling. PhD Thesis.

De Caro, M., Perico, R., Crosta, G.B., Frattini, P., Volpi, G., 2020. A regional-scale conceptual and numerical groundwater flow model in fluvio-glacial sediments for the Milan Metropolitan area. J. Hydrol. Reg. Stud. 29, 100683 https://doi.org/10.1016/j.ejrh.2020.100683.

De Luca, D.A., Destefanis, E., Forno, M.G., Lasagna, M., Masciocco, L., 2014. The genesis and the hydrogeological features of the Turin Po Plain fontanili, typical lowland springs in Northern Italy. Bull. Eng. Geol. Environ. 73, 409–427. https://doi.org/10.1007/s10064-013-0527-y.

di Milano, CittàMetropolitana, 2019. SIA - Sistema Informativo Ambientale. URL http://ambiente.provincia.milano.it/sia (Accessed 7.2.19).

Di Sipio, E., Galgaro, A., Destro, E., Teza, G., Chiesa, S., Giaretta, A., Manzella, A., 2014. Subsurface thermal conductivity assessment in Calabria (southern Italy): a regional case study. Environ. Earth Sci. 1383–1401. https://doi.org/10.1007/s12665-014-3277-7.

ENEA, 2018. Rapporto Annuale Efficienza Energetica.

Epting, J., Huggenberger, P., 2013. Unraveling the heat island effect observed in urban groundwater bodies - Definition of a potential natural state. J. Hydrol. (Amst.) 501, 193–204. https://doi.org/10.1016/j.jhydrol.2013.08.002.

Epting, J., Müller, M.H., Genske, D., Huggenberger, P., 2018. Relating groundwater heat-potential to city-scale heat-demand: a theoretical consideration for urban groundwater resource management. Appl. Energy 228, 1499–1505. https://doi.org/10.1016/j.apenergy.2018.06.154.

European Climate Foundation, 2010. Roadmap 2050 a Practical Guide to a Prosperous Low-carbon Europe. Technical Analysis, Policy. https://doi.org/10.2833/10759.

European Commission, 2018. Directive (EU) 2018/2001 of the European Parliament and of the Council on the promotion of the use of energy from renewable sources. Off. J. Eur. Union.

EUROSTAT, 2019. Energy Statistics - Price of Natural Gas and Electricity. URL https://ec.europa.eu/eurostat/web/energy/data/database (Accessed 6.1.19).

Galgaro, A., Di Sipio, E., Teza, G., Destro, E., De Carli, M., Chiesa, S., Zarrella, A., Emmi, G., Manzella, A., 2015. Empirical modeling of maps of geo-exchange potential for shallow geothermal energy at regional scale. Geothermics 57, 173–184. https://doi.org/10.1016/j.geothermics.2015.06.017.

García-Gil, A., Vázquez-Suñe, E., Alcaraz, M.M., Juan, A.S., Sánchez-Navarro, J.Á., Montlleó, M., Rodríguez, G., Lao, J., 2015. GIS-supported mapping of low-temperature geothermal potential taking groundwater flow into account. Renew. Energy 77, 268–278. https://doi.org/10.1016/j.renene.2014.11.096.

Garzanti, E., Vermeli, G., Andò, S., 2011. Paleogeographic and paleodrainage changes during Pleistocene glaciations (Po Plain, northern Italy). Earth-Sci. Rev. 105, 25–48.

GSE, 2018. Gestore dei Servizi Energetici - Rapporto Statistico energia da fonti rinnovabili anno 2017 [2017 statistical report on renewable energy].

ISPRA, Regione Lombardia, 2016. Note Illustrative della Carta Geologica d'Italia - Foglio 118 Milano.

ISTAT, 2019. Dati del censimento della popolazione e delle abitazioni 2011 (Italian population census). URL http://datiopen.istat.it/ (Accessed 7.2.19).

Kavanaugh, S.P., Rafferty, K., 2014. Geothermal Heating and Cooling: Design of Ground-Source Heat Pump Systems (ASHRAE).

Kurylyk, B.L., MacQuarrie, K.T.B., Caissie, D., McKenzie, J.M., 2015. Shallow groundwater thermal sensitivity to climate change and land cover disturbances: derivation of analytical expressions and implications for stream temperature modeling. Hydrol. Earth Syst. Sci. Discuss. 19, 2469–2489. https://doi.org/10.5194/hess-19-2469-2015.

Lippman, M.J., 1980. Ground Water Use for Cooling: Associated Aquifer Temperature Changes.

Lombardia, A.R.P.A., 2019. Meteo Lombardia - Dati Misurati. URL www.arpalombardia.it/siti/arpalombardia/meteo/richiesta-dati-misurati (Accessed 7.2.19).

Lund, J.W., Boyd, T.L., 2016. Direct utilization of geothermal energy 2015 worldwide review. Geothermics 60, 66–93. https://doi.org/10.1016/j.geothermics.2015.11.004.

Mueller, M.H., Huggenberger, P., Epting, J., 2018. Combining monitoring and modelling tools as a basis for city-scale concepts for a sustainable thermal management of urban groundwater resources. Sci. Total Environ. 627, 1121–1136. https://doi.org/10.1016/j.scitotenv.2018.01.250.

Perego, R., Pera, S., Galgaro, A., 2019. Techno-economic mapping for the improvement of shallow geothermal management in Southern Switzerland. Energies 12, 279. https://doi.org/10.3390/en12020279.

Pichierri, M., Bonafoni, S., Biondi, R., 2012. Satellite air temperature estimation for monitoring the canopy layer heat island of Milan. Remote Sens. Environ. 127, 130–138. https://doi.org/10.1016/j.rse.2012.08.025.

Regione Lombardia, 2010. Regolamento Regionale n.7 15/02/2010.

Regione Lombardia, 2017. Deliberazione 6203 (08/02/2017), L.R. 38/2015, D.LGS 152 03/04/2006.

Regione Lombardia, 2019a. Registro Regionale Sonde Geotermiche. URL http://www.rinnovabililombardia.it/rsg (Accessed 7.2.19).

Regione Lombardia, 2019b. Geoportale della regione Lombardia. URL http://www.geoportale.regione.lombardia.it/ (accaccessed 9.2.19).

Regione Lombardia, 2019c. Carta Geoenergetica Regionale. URL http://www.rinnovabililombardia.it/cartageoenergetica (Accessed 7.25.19).

Regione Lombardia, 2019d. CURIT - Catasto Impianti Termici. URL www.curit.it (Accessed 9.20.19).

Regione Lombardia, ENI Division Agip, 2002. Geologia degli acquiferi Padani della Regione Lombardia. Selca (Firenze).

Regione Lombardia - CASPITA, 2019. Banca dati geologica del sottosuolo. URL http://www.geoportale.regione.lombardia.it/download-dati (Accessed 7.2.19).

Rubel, F., Brugger, K., Haslinger, K., Auer, I., 2017. The climate of the European Alps: shift of very high resolution Köppen-Geiger climate zones 1800-2100. Meteorol. Zeitschrift 26, 115–125. https://doi.org/10.1127/metz/2016/0816.

Saner, D., Juraske, R., Kübert, M., Blum, P., Hellweg, S., Bayer, P., 2010. Is it only CO 2 that matters? A life cycle perspective on shallow geothermal systems. Renew. Sustain. Energy Rev. 14, 1798–1813. https://doi.org/10.1016/j.rser.2010.04.002.

Self, S.J., Reddy, B.V., Rosen, M.A., 2013. Geothermal heat pump systems: status review and comparison with other heating options. Appl. Energy 101, 341–348. https://doi.org/10.1016/j.apenergy.2012.01.048.

Signorelli, S., Kohl, T., 2004. Regional ground surface temperature mapping from meteorological data. Glob. Planet. Change 40, 267–284. https://doi.org/10.1016/j.gloplacha.2003.08.003.

Stauffer, F., Bayer, P., Blum, P., Molina-Giraldo, N., Kinzelbach, W., 2013. Thermal use of Shallow Groundwater, Thermal Use of Shallow Groundwater. https://doi.org/10.1201/b16239.

Unione Geotermica Italiana, 2017. Growth Forecasts of Geothermal Energy in Italy 2016-2030, With Projections to 2050. UGI.

VDI 4640, 2001. German Guidelines: Thermal Use of the Underground. VDI-RICHTLINIEN - Therm. Use Undergr. Gr. Source Heat Pump Syst..

Viesi, D., Galgaro, A., Visintainer, P., Crema, L., 2018. GIS-supported evaluation and mapping of the geo-exchange potential for vertical closed-loop systems in an Alpine valley, the case study of Adige Valley (Italy). Geothermics 71, 70–87. https://doi.org/10.1016/j.geothermics.2017.08.008.

Zhu, K., Blum, P., Ferguson, G., Balke, K.-D., Bayer, P., 2011. The geothermal potential of urban heat islands. Environ. Res. Lett. 6, 019501 https://doi.org/10.1088/1748-9326/6/1/019501.